Seeking dark matter with γ-ray attenuation

José Luis Bernal,[1] Andrea Caputo,[2,3] Gabriela Sato-Polito,[1] Jordan Mirocha,[4] and Marc Kamionkowski[1]

[1]*William H. Miller III Department of Physics and Astronomy, Johns Hopkins University, 3400 North Charles Street, Baltimore, Maryland 21218, USA*

[2]*School of Physics and Astronomy, Tel-Aviv University, Tel-Aviv 69978, Israel*

[3]*Department of Particle Physics and Astrophysics, Weizmann Institute of Science, Rehovot 7610001, Israel*

[4]*McGill University, Department of Physics and McGill Space Institute, 3600 Rue University, Montréal, Quebec City, Canada H3A 2T8*

(Received 8 September 2022; revised 24 February 2023; accepted 11 May 2023; published 24 May 2023)

The flux of high-energy astrophysical γ rays is attenuated by the production of electron-positron pairs from scattering off of extragalactic background light (EBL). We use the most up-to-date information on galaxy populations to compute their contributions to the pair-production optical depth. We find that the optical depth inferred from γ-ray measurements exceeds that expected from galaxies at the $\sim 2\sigma$ level. If the excess is modeled as a frequency-independent re-scaling of the standard contribution to the EBL from galaxies, then an excess (an overall 14–30% increase of the EBL) is favored over the null hypothesis of no excess at the 2.7σ level. If the frequency dependence of the excess is instead modeled as a two-photon decay of a dark-matter axion, then the excess is favored over the null hypothesis at the 2.1σ confidence level. While we find no evidence for a dark-matter signal, the analysis sets the strongest current bounds on the photon-axion coupling over the 8–25 eV mass range. This work highlights the sensitivity of γ-ray optical depth measurements to ALPs, which is expected to improve with new observatories and better EBL determinations from future observations.

DOI: 10.1103/PhysRevD.107.103046

I. INTRODUCTION

The extragalactic background light (EBL) is defined as the integrated flux aggregating all emission over cosmic times [1]. Direct measurements are challenging due to the overwhelming contamination from foregrounds, which makes it necessary to resort to indirect observational or theoretical determinations to get a census of the populations of emitters. In addition to astrophysical emissions, exotic contributions may be present, arising from a potential connection between dark matter and Standard Model particles, for instance.

Dark matter is a key component of our understanding of the Universe, but a microscopic model backed by observational and experimental evidence is yet to be found [2]. The axion—a pseudo-Nambu-Goldstone boson initially proposed to solve the strong-CP problem—and axionlike particles (ALPs) are natural dark-matter candidates [3–9], with rich phenomenology that enables a variety of search strategies [10,11]. The coupling between ALPs and photons causes oscillations in the presence of magnetic fields, but also allows ALPs to undergo a monochromatic decay into two photons with energy $m_a c^2/2$, where m_a is the ALP mass. The decay rate depends on the ALP-photon effective coupling $g_{a\gamma}$ as $\Gamma_a = (m_a c^2)^3 g_{a\gamma}^2/32h$, where c is the speed of light and h is the Planck constant. Searches for signatures of ALP decays span a vast energy range (see e.g., [12–38]). Here we seek their contributions to the EBL, focusing on indirect EBL determinations from γ-ray attenuation.

As γ rays propagate through a bath of low-energy photons they are absorbed through electron-positron pair production [39,40]. Joint analyses of the observed blazar spectra allow the attenuation to be determined as function of source redshift and observed γ-ray energy [41]. Assuming there is no secondary production of γ rays due to undeflected cosmic rays in the jet [42–44], these measurements can be used to infer the EBL intensity between the infrared and near ultraviolet as a function of redshift [45–48]. Moreover, using independent determinations of the EBL, they can also be used to constrain the expansion history of the Universe [49], study Pop III stars [50], and test fundamental physics [51], among others. In particular, γ-ray attenuation measurements are sensitive to axion-photon oscillations: using the EBL as a "screen" for a "light through a wall" experiment [52–55] yields competitive bounds on the ALP-photon coupling for $10^{-2} - 10^{2}$ neV masses (see e.g., [56–61]). Nonetheless, γ-ray attenuation is also sensitive to multielectronvolt ALP decays through their contribution to the EBL, as proposed in Refs. [62–64].

Revisiting exotic contributions to the EBL is timely. A recent measurement of the cosmic optical background performed by the New Horizons spacecraft yields a $\sim 4\sigma$ significant excess with respect to the expected flux from

deep galaxy counts [65,66]. Furthermore, indirect determinations of the EBL [46,48] lie above the inferred EBL from galaxy populations over a much wider frequency range [67]. These excesses may be due to unaccounted for astrophysical contributions, but the New Horizons's excess may also be explained with ALP dark matter [68].

Electronvolt-scale ALPs are hard to probe with current strategies, which motivates the development of new probes. Forthcoming line-intensity mapping experiments are expected to significantly improve sensitivities in this region of the parameter space [69–71]. Contributing to this endeavor, we present an independent probe for the dark-matter ALP using high-energy γ rays. We significantly improve over preliminary attempts [63,64], performing a systematic analysis of γ-ray absorption of a considerably larger sample of sources across redshift and observed energies, and confront it with a comprehensive observational and theoretical determination of the astrophysical EBL.

This paper is structured as follows. We review the computation of the γ-ray optical depth and introduce the contributions considered in this work in Sec. II; we describe our analysis and present our results in Sec. III; and conclude in Sec. IV. Further details on the astrophysical model for the standard contributions to the EBL considered in this work (Appendix A), the likelihood used in the analysis (Appendix B), and null tests to inform our conclusions can be found in the Appendix C.

II. γ-RAY OPTICAL DEPTH

The optical depth is the line-of-sight integral of the inverse of the mean free path l of all the interactions that a γ ray encounters as it travels from the source to us: $\tau = c\int_0^{z_s} \mathrm{d}z l^{-1}/[H(1+z)]$, where z_s is the source redshift, and H is the Hubble parameter. We refer to observed energies and rest-frame energies at a given redshift as E and $\epsilon \equiv E(1+z)$, respectively. For a γ ray with observed energy E_γ in a bath of EBL photons, electron-positron pair production occurs above the EBL photon energy threshold,

$$\epsilon_{\min} = \frac{2m_e^2c^4}{E_\gamma(1+z)(1-\mu)}, \tag{1}$$

where m_e is the electron mass and μ is the cosine of the angle of incidence between the two photons. The cross section for the process is [40]

$$\sigma_{\gamma\gamma}(\beta) = \frac{3\sigma_{\mathrm{T}}}{16}(1-\beta^2)\times\left[2\beta(\beta^2-2)+(3-\beta^4)\ln\left(\frac{1+\beta}{1-\beta}\right)\right], \tag{2}$$

where σ_T is the Thomson cross section and $\beta^2 = 1–2m_e^2c^4/(\epsilon\epsilon_\gamma(1-\mu))$ is the electron velocity in the center-of-mass frame. Assuming an isotropic gas of low-energy background photons with specific number density $\mathrm{d}n/\mathrm{d}\epsilon$ in proper coordinates, the inverse of the mean free path is

$$l^{-1} = \int_0^\infty \mathrm{d}\epsilon \frac{\mathrm{d}n}{\mathrm{d}\epsilon}\int_{-1}^{1}\mathrm{d}\mu\frac{(1-\mu)}{2}\sigma_{\gamma\gamma}\Theta(\epsilon-\epsilon_{\min}), \tag{3}$$

where Θ is the Heaviside function.[1] The angular integral peaks as ϵ tends to $\epsilon'_{\min}$, which corresponds to $\epsilon_{\min}$ with $\mu=-1$. The number density can also be obtained from the specific intensity per unit energy I_ϵ in comoving coordinates as $\mathrm{d}n/\mathrm{d}\epsilon = 4\pi(1+z)^3 I_\epsilon/(c\epsilon)$.[2] As a reference, the minimum energy that ever contributes to the attenuation is $\epsilon'_{\min} \simeq 1.3\ \mathrm{eV}(100\ \mathrm{GeV}/E_\gamma)(2/(1+z_s))$.

A. Contributions to the EBL

The proper ALP-sourced photon number density per energy interval at a given redshift is the aggregate of all the decays at earlier times that redshift to the energy of interest:

$$\begin{aligned}\left(\frac{\mathrm{d}n}{\mathrm{d}\epsilon}\right)^{\mathrm{dec}} &= \frac{\Omega_a\rho_{\mathrm{c}}c^2\Gamma_a(1+z)^3}{m_ac^2/2} \\ &\times\int_z^\infty\frac{\mathrm{d}z'}{H(z')(1+z')}\delta_D\left(\epsilon-\frac{m_ac^2(1+z)}{2(1+z')}\right) \\ &= \frac{2\Omega_a\rho_{\mathrm{c}}c^2\Gamma_a(1+z)^3}{m_ac^2\epsilon H(z_*)}\Theta(z_\star-z),\end{aligned} \tag{4}$$

where δ_D is the Dirac delta function, Ω_a and ρ_{c} are the ALP density parameter and the critical density today, respectively, and $z_* \equiv m_ac^2(1+z)/(2\epsilon)-1$ is the redshift of decay that contributes to the photon energy and redshift of interest. We assume that ALPs make up all of the dark matter and, for the energies of interest, we can safely consider that decay photons have a Dirac delta-function profile [14]. The condition $z_\star > z$ is equivalent to setting the rest-frame energy as the upper limit in the integral over ϵ in Eq. (3).

In order to quantitatively determine the contribution from ALP decays to the γ-ray attenuation we need to budget standard contributions to the EBL from astrophysical sources. The EBL can be directly measured (see e.g., Refs. [73–76]), though foreground contamination hinders this approach (motivating measurements from the outskirts of the solar system [65,66,77]). Instead, we reconstruct the EBL using observational and theoretical information. We distinguish three components: emission from galaxies at $z<6$, emission from galaxies at $z>6$, and the intrahalo light (IHL)—emission from a faint population of stars tidally removed from galaxies [78–80]. The cosmic

[1]We further simplify this equation following Ref. [72], limiting the energy integral to values above $\epsilon'_{\min}$ and computing the angular integral analytically, changing variable from μ to β.

[2]Note that $\lambda I_\lambda = \epsilon I_\epsilon$.

microwave background photons have energies too low to contribute to the optical depth of the blazars of interest.

We use the determination of the EBL sourced from galaxies at $z < 6$ from Ref. [67], which is fairly consistent with alternative semianalytic, phenomenological and empirical studies (see e.g., Refs. [81–86]). We reweight specific comoving luminosity densities $j_\nu(z)$ inferred from multiwavelength HST/CANDELS surveys [87,88] to match our fiducial cosmology.[3] We use the code ARES[4] [90] to model the contribution from stars at $z > 6$, using an empirical model for Pop II star-forming galaxies calibrated with observations of the ultraviolet luminosity function [91]. We also consider the contribution from Pop III stars, following the modeling from Ref. [92]. In each case, we also include x-ray emission representative of high-mass x-ray binary systems, though these sources contribute little to the γ-ray optical depth. We adopt extreme cases to be conservative regarding uncertainties. Finally, we model the IHL luminosity density with a power-law dependence in mass and redshift [78], assuming a spectral energy distribution similar to old elliptical galaxies [93]. We take results from Ref. [94] to set the fiducial contribution and its uncertainties. We compute the flux from each astrophysical contribution i in comoving coordinates as function of redshift,

$$\lambda I_{\lambda,i}(\lambda, z) = \frac{c^2}{4\pi\lambda}\int_{z_0}^{z_{\max}} \mathrm{d}z' \frac{j_{\nu',i}\left(\frac{\lambda(1+z)}{1+z'}, z'\right)}{H(z')(1+z')}, \qquad (5)$$

where λ is the rest-frame wavelength at redshift z, ν' is the rest-frame frequency at z', and $z_0 = z(6)$ and $z_{\max} = 6(60)$ for the contributions from galaxies at $z < 6$ and the IHL (from galaxies at $z > 6$). We use the resulting flux as function of redshift to compute the optical depth due to each contribution, propagating the uncertainties accordingly. The interested reader can find more details about the computation of the astrophysical contributions in Appendix A.

In order to provide an idea of the shape and magnitude of each contribution, we compare the various photon number densities at $z = 0.5$ and 1.5, and their corresponding optical depths for γ rays with observed energies of 50 and 100 GeV in Fig. 1. The ALP-sourced photon density grows with ϵ, contrary to astrophysical photons, since for the same ALP mass lower energies correspond to decays occurring at higher redshifts, for which the time interval, and hence the total flux, is smaller. The dependence on redshift is mostly a small change in amplitude, with an additional small tilt and shift in the astrophysical contributions. As expected, the contribution from galaxies at $z < 6$ vastly dominates the EBL. The gap between low and high-energy EBL photons

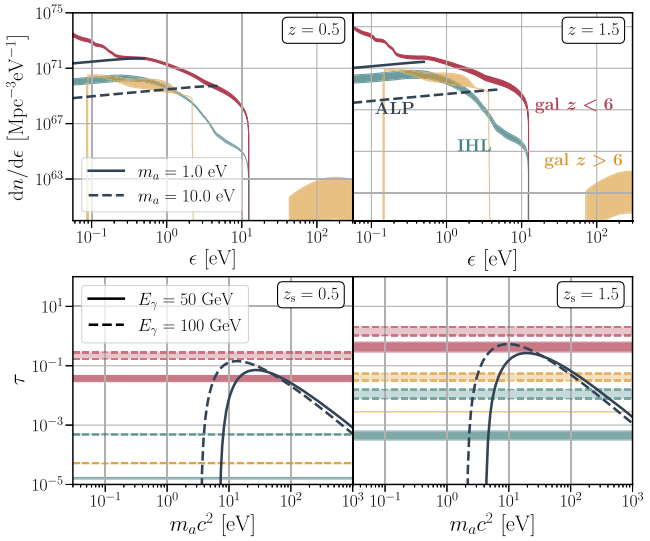

FIG. 1. Photon number density in proper coordinates (top panels) and γ-ray optical depth for observed energies of 50 and 100 GeV (bottom panels), distinguishing contributions from galaxies at $z < 6$, $z > 6$, and the IHL (red, orange and blue, respectively, shaded bands denoting the 68% confidence level uncertainties) and ALP decays for a decay rate of 3×10^{-24} s^{-1} (solid lines), similar to the best fit obtained in this work.

for astrophysical sources at $z > 6$ is due to neutral hydrogen absorption. The dependence of the optical depth on source redshift is similar, with a slight shift toward smaller masses for higher source redshifts.

III. ANALYSIS AND RESULTS

We can confront now the predicted optical depth due to ALP decays with attenuation measurements. We take public optical depth measurements obtained from the analysis of 739 blazars observed by FermiLAT [46] and 38 blazars observed by ground-based Cherenkov observatories [48]. These amount to optical depth measurements in 12 z_s bins for $E_\gamma \in [10 - 10^3]$ GeV, and in 2 z_s bins for $E_\gamma \in [0.1\text{–}20]$ TeV. We combine these measurements with the inferred optical depth and uncertainty from astrophysical sources to generate a sample of residual optical depth $\tau_{\rm res}$ to be contributed from unaccounted-for sources (i.e., the ALP decays in this case). We remove lower-limit measurements from our sample since they do not set any limit to the additional contributions. Further details on the computation of $\tau_{\rm res}$ can be found in Appendix B. We find $\tau_{\rm res} > 0$ in some cases, which is consistent with previous results comparing EBL determinations with the inference from γ-ray attenuation [67].

We follow Ref. [46] and assume a Gaussian likelihood for $\tau_{\rm res}$. We adopt flat priors on $\log_{10}(m_a c^2/\mathrm{eV}) \in [-1, 2]$ and $\log_{10}(\Gamma_a/\mathrm{s}^{-1}) \in [-28, -20]$. We evaluate the unnormalized posterior in a fine grid in $\log_{10}(m_a c^2/\mathrm{eV})$ and $\log_{10}(\Gamma_a/\mathrm{s}^{-1})$, and derive the posterior from the $\Delta\chi^2$ with

[3]Full *Planck* dataset best-fit parameters assuming ΛCDM [89].
[4]https://github.com/mirochaj/ares.

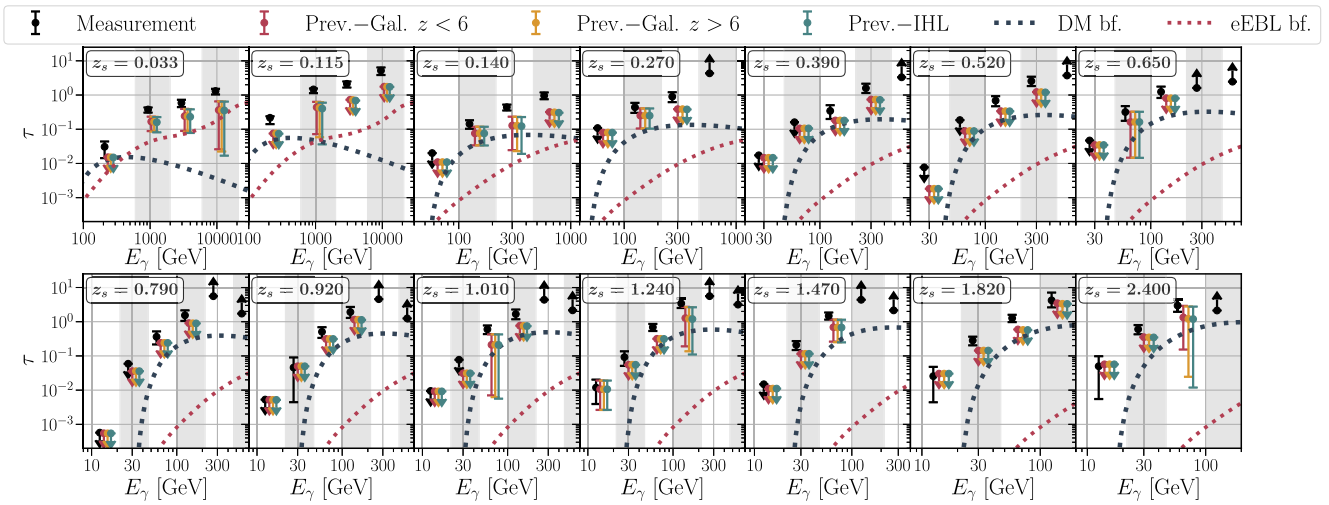

FIG. 2. Measured and residual γ-ray optical depths binned in source redshift and observed γ-ray energy. We show residual optical depths as we cumulatively subtract astrophysical components (as indicated in the legend, each entry is the previous minus the indicated component). Dark blue dotted lines show the best-fit results for the contributions from ALP decays. We also show the best fit results for the case with additional extragalactic background with red dotted lines.

respect to the best-fit χ^2.[5] We neglect neutral hydrogen absorption for ALP masses above 20.4 eV. The absorption of the photons produced in these decays would require higher decay rates to contribute the same to the EBL. However, as shown below, this region of the parameter space is better constrained by other probes, so that this choice does not affect our conclusions.

The excess in optical depth can be explained with ALP decays, with best fit $m_a c^2 = 9.1$ eV and $\Gamma_a = 2.5 \times 10^{-24}\ \mathrm{s}^{-1}$, which corresponds to $g_{a\gamma} = 2.1 \times 10^{-11}\ \mathrm{GeV}^{-1}$. We find that the contributions from ALP decays are preferred over the null hypothesis (no additional optical depth) at 2.1σ significance ($p-$value $= 0.038$). We show τ_{meas}, τ_{res} and the predicted contributions from ALPs for the best fit in Fig. 2. The ALP contributions provide a very good fit for τ_{res}, with the exception of the measurements at $z_s = 0.033$.

Our results can also easily be rescaled to smaller abundances of ALPs modifying Eq. (4) accordingly. For the coupling and masses of interest, the correct dark-matter relic abundance can be obtained via the misalignment mechanism [3–5], although only in nonstandard cosmology scenarios [95–97] or specific photophilic models where the ALP-photon coupling is enhanced, while keeping a relatively large decay constant [98].

We also explore a simplified null test. We consider a separate case to explain the optical depth excess with a boosted contribution from galaxies at $z < 6$: we multiply such contribution by a constant factor $(1 + F_{\mathrm{eEBL}})$,[6] adopting a flat prior on $\log_{10} F_{\mathrm{eEBL}} \in [-3, 1]$. We find $F_{\mathrm{eEBL}} = 0.22 \pm 0.08$ at 68% confidence level, which fits well the first bins in z_s, but fails for blazars at higher redshift for which τ_{res} is not an upper limit. $F_{\mathrm{eEBL}} > 0$ is preferred at 2.7σ ($p-$value $= 6.7 \times 10^{-3}$). The $\Delta\chi^2$ between the best fits in this and the ALP cases favors the former with marginal significance. If the first z_s bin is removed we find $\Delta\chi^2 = -2.9$, favoring ALP decays, with approximately the same best-fit parameters for the ALP decay than before (and same significance of detection against the null hypothesis), but 0.17 ± 0.09 for F_{eEBL} at 68% confidence level. Further discussion and null tests can be found in Appendix C.

We compare our results for the ALP decay rate with the current strongest bounds over the relevant mass range in Fig. 3. We include bounds from the helioscope CAST [99], from spectroscopic observations of the galaxy clusters Abell 2667 and 2390 with VIMOS [100] and the dwarf spheroidal galaxy Leo T with MUSE [101], the study of the stellar cooling in globular clusters [102,103], cosmic microwave background spectral distortions measured with COBE/FIRAS [31], radiative gas cooling rates of Leo T [28], and HST angular power spectrum [104]; and forecast sensitivities of line-intensity mapping [70].[7] We do not include outdated constraints from observations of the optical and near-infrared background [105] and instead

[5]Exploring the parameter space of $\log_{10}(\Gamma_a/\mathrm{s}^{-1})$ and $\log_{10}(g_{a\gamma}/\mathrm{GeV}^{-1})$ returns the same posterior, since the likelihood $\mathcal{L}(\log_{10}(g_{a\gamma}/\mathrm{GeV}^{-1}), \log_{10}(m_a c^2/\mathrm{eV})) = 2\mathcal{L}(\log_{10}(\Gamma_a/\mathrm{s}^{-1}), \log_{10}(m_a c^2/\mathrm{eV}))$, which yields the same $\Delta\chi^2$.

[6]Note that we only increase the mean contributions and do not vary the error bars that go into the computation of τ_{res}.

[7]We include forecasts using the voxel intensity distribution (VID, an estimator for the probability distribution function of the line intensity within a voxel), and the power spectrum (PS).

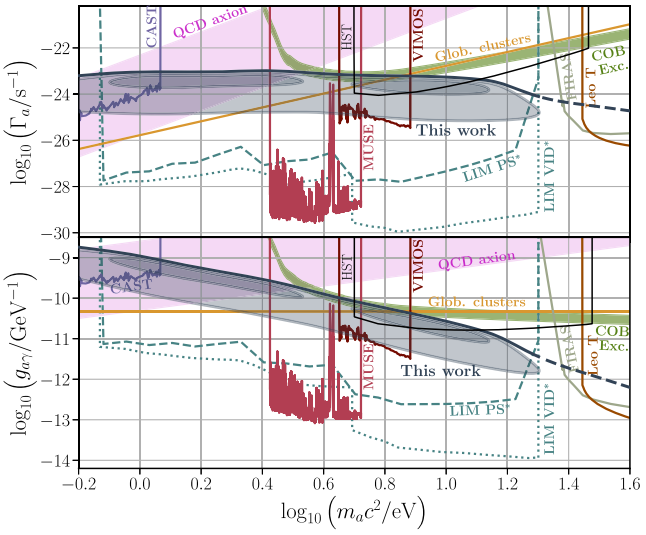

FIG. 3. 68%, 95%, and 99% confidence level constraints on the ALP parameters from γ-ray attenuation (dark blue contours, dashed lines denoting the masses that are affected by neutral hydrogen absorption), along with current strongest 95% confidence level bounds and preferred region to explain the COB excess, and the QCD axion band.

add the preferred parameter values to explain the cosmic optical background excess [68]. The bimodal distribution is produced by the difficulty to fit the local and high z_s measurements at the same time (see Appendix C).

The fact that the optical depth excess may also be explained by additional EBL from galaxies at $z < 6$ may point to a scenario where both additional components contribute to the EBL. The exploration of this hypothesis requires a more detailed modeling for the additional astrophysical EBL and is left for future work. Therefore, the hint found in this work shall be confirmed by subsequent studies and additional, independent probes of ALP, and we prefer to interpret this result as an upper bound in the ALP-photon coupling and a motivation for further exploration of this region of the parameter space.

IV. CONCLUSIONS

γ-ray attenuation returns the strongest 3σ bound to date on the effective ALP-photon coupling on the 8–25 eV mass range, improving current bounds by up to more than an order of magnitude. These results rule out most of the parameter space that may explain the cosmic optical background excess, leaving a small window at $m_a c^2 \sim 8$ eV. However, note that Ref. [68] does not include contributions from IHL and galaxies at $z > 6$, which may push the viable parameter combinations to lower effective couplings, increasing the compatibility with this work.

Our analysis is significantly more sensitive to ALP contributions than the study from Ref. [64], based on fitting a bump feature in the spectrum of a single blazar. This is because we use optical-depth measurements from almost 800 blazars, making our study more robust statistically and regarding uncertainties in the intrinsic spectra of the blazars. We rule out most of the viable favored parameter space reported in Ref. [64] and we find potential preference for lower couplings.

γ-ray attenuation as a probe for ALPs or other nonstandard contributions to the EBL has great potential to improve in the near future. Existing γ-ray satellites and ground Cherenkov telescopes like Fermi-LAT and HAWC,[8] HESS,[9] MAGIC,[10] or VERITAS[11] will keep improving the measurements and increasing the sensitivity to the EBL, while forthcoming facilities such as CTA [106] will bring dramatic improvements. On the other hand, improved observations of the EBL such as a reassessment of HST data [107] or observations with SPHEREx [108] and JWST,[12] will reduce uncertainties in the EBL determination and increase the precision and robustness of analyses like this one. Furthermore, line-intensity mapping observations will distinguish between different potential sources for exotic lines [70,109], while a non detection would imply that any additional contribution must have a broad spectrum, increasing the characterization of any non-accounted for contributions to the EBL and γ-ray attenuation.

ACKNOWLEDGMENTS

J. L. B. is supported by the Allan C. and Dorothy H. Davis Fellowship. A. C. is supported by the Foreign Postdoctoral Fellowship Program of the Israel Academy of Sciences and Humanities and also acknowledges support from the Israel Science Foundation (Grant 1302/19) and the European Research Council (ERC) under the EU Horizon 2020 Programme (ERC-CoG-2015-Proposal n. 682676 LDMThExp). G. S. P. was supported by the National Science Foundation Graduate Research Fellowship under Grant No. DGE1746891. M. K. was supported by NSF Grant No. 2112699 and the Simons Foundation.

APPENDIX A: ASTROPHYSICAL EBL MODEL

Here we provide more details on the theoretical models used to determine the contributions to the EBL from galaxies at $z > 6$ and the IHL.

1. Galaxies at $z > 6$

Our model for the contribution to the EBL from galaxies at $z > 6$ has two components. In order to be conservative, we adopt two extreme cases, and take the envelope of the

[8] https://www.hawc-observatory.org/.
[9] https://www.mpi-hd.mpg.de/hfm/HESS/.
[10] https://magic.mpp.mpg.de/.
[11] https://veritas.sao.arizona.edu/.
[12] https://www.jwst.nasa.gov/.

resulting minimum and maximum EBL as our lower and higher value uncertainties.

First, we include an empirically-calibrated model for Pop II star-forming galaxies [91], which relates the star-formation rate to the accretion rate of dark matter halos, and infers the star formation efficiency through fits to high-z galaxy luminosity functions from [110]. We use the BPASS version 1.0 single-star models [111] to generate our model galaxy spectrum, assuming solar metallicity, no attenuation from dust, and that stars have been forming at a constant rate for 100 Myr. This is a reasonable approximation for the rest-ultraviolet portion of high-z galaxy spectra, which is the most relevant for the γ-ray opacity from the EBL.

We also include a contribution from Pop III stars, which form in low-mass "minihalos" with virial temperatures below the atomic cooling threshold. We either do not account for contributions from Pop III stars or assume that Pop III stars dominate the cosmic star-formation rate density until $z \simeq 15$ and are extinct by $z \simeq 10$. This scenario is achieved assuming a simple parametrization [92], in which each halo forms Pop III stars for 250 Myr before transitioning to Pop II star formation. Pop III stars are assumed to be massive, $\gtrsim 100 M_\odot$ stars with hard spectra, comparable to a black body at 10^5 K [112]. Such a model will be testable with forthcoming observations by SPHEREx [113].

In addition, we assume that each stellar source population described above is also accompanied by high-mass x-ray binaries, which contribute to the x-ray background. For these sources, we assume a multicolor disk spectrum [114], with no intrinsic attenuation. We consider cases in which the relationship between x-ray emission and the star-formation rate is similar to the local relation [115], as well as a case where it is boosted by a factor 10^3 with respect to the local relation. In both cases, the contribution to the opacity from the EBL is negligible, since the range of energies of the redshifted x-ray photons do not annihilate γ-ray photons efficiently.

We model these high-z sources and their contribution to the EBL using the publicly-available ARES code [90]. Note that the lowest energy of the $z > 6$ contribution is set by the lowest energy considered within ARES, which is the minimum photon included in the BPASS library $\simeq$0.4 eV. Nevertheless, this energy is always below $\epsilon'_{\rm min}$, hence not affecting the results.

2. Intrahalo light

Diffuse intrahalo emission, usually referred to as intrahalo light (IHL), may come from tidally stripped stars during galaxy mergers, with aggregated surface brightness low enough to challenge resolved observations [116]. The fraction of stripped stellar mass depends on the halo mass, with heavier halos expected to host larger fractions of diffuse intra-halo emission than their lighter counterparts. We follow the parametric model from Refs. [94,117]. The specific luminosity density at redshift z and rest-frame wavelength λ can be computed using the halo mass function $\mathrm{d}n_{\rm h}/\mathrm{d}M$ as

$$j_{\lambda,\rm IHL}(\lambda, z) = \int_{M_{\rm min}}^{M_{\rm max}} \mathrm{d}M \frac{\mathrm{d}n_{\rm h}}{\mathrm{d}M} L_{\lambda,\rm IHL}(M, z), \quad \text{(A1)}$$

where we use the halo mass function from Ref. [118], we assume $M_{\rm min} = 10^9 M_\odot/h$ and $M_{\rm max} = 10^{13} M_\odot/h$, where $h = H_0/(100\ \mathrm{km/s/Mpc})$ in this context, and $L_{\lambda,\rm IHL}$ is the intrahalo light specific luminosity emitted by a halo of mass M, given by

$$L_{\lambda,\rm IHL}(M, z) = f_{\rm IHL}(M) L_{2.2}(M)(1+z)^\alpha S_{\lambda,2.2}(\lambda), \quad \text{(A2)}$$

where $L_{2.2} \equiv L_0/(2.2\ \mu\mathrm{m})$ is the total halo luminosity at 2.2 μm at $z = 0$, with L_0 given by [119]

$$L_0 = 5.64 \times 10^{12} h_{70}^{-2} \left(\frac{M}{2.7 \times 10^{14} h_{70}^{-1} M_\odot}\right)^{0.72} L_\odot, \quad \text{(A3)}$$

where $h_{70} = H_0/(70\ \mathrm{km/s/Mpc})$. In Eq. (A2), α controls the redshift evolution of the luminosity and $f_{\rm IHL}$ is the fraction of the total halo luminosity coming from IHL. We parametrize $f_{\rm IHL}$ with a power law in mass

$$f_{\rm IHL} = A_{\rm IHL} \left(\frac{M}{10^{12} M_\odot}\right)^\beta. \quad \text{(A4)}$$

Finally, $S_{\lambda,2.2} \equiv S_\lambda/S_{2.2}$ is the spectral energy distribution of the IHL normalized to be 1 at 2.2 μm. We assume S_λ to be similar to old elliptical galaxies, comprised of red stars [93]. In practice, we use the template for an elliptical galaxy of age 13 Gyr from the *SWIRE* library [120]. Once we have computed j_λ, we transform it to j_ν and compute the contributions to the EBL using Eq. (5).

We follow the results of Ref. [94], which assumes a fixed index for the mass power law to 0.1 (in agreement with the best fit to the near-infrared background power spectrum, $\beta = 0.094 \pm 0.005$ [78]), and finds the index of the redshift power law and the $\log_{10} A_{\rm IHL}$ completely anticorrelated, and fairly uncorrelated with other contributions. We set $\log_{10} A_{\rm IHL} = \{-3.35, -3.23, -3.09\}$ and $\alpha = \{0.1, 1, 1.5\}$ as the low, mean and high values for our estimation, according to the reported 68% confidence level constraints in Ref. [94].

APPENDIX B: LIKELIHOOD

In this appendix we provide further detail about the likelihood we use for the residual optical depth $\tau_{\rm res}$. Let us first describe how we obtain $\tau_{\rm res}$ for each source redshift $z_{\rm s}$ and observed energy E_γ from the measured optical depth $\tau_{\rm meas}$ and the predicted contributions to the optical depth τ_k from each component of the astrophysical EBL (gal. $z < 6$, gal. $z > 6$, and IHL), indexed by k. We index the $z_{\rm s}$ and E_γ

values with i and j, respectively, so that $\tau(z_s^{(i)}, E_\gamma^{(j)}) \equiv \tau^{(ij)}$. As discussed in the main body of the article, we discard lower-limit measurements of $\tau_{\rm meas}$, and distinguish between actual measurements and only upper limits for $\tau_{\rm meas}$. If $\tau_{\rm meas}^{(ij)}$ is detected, we compute $\tau_{\rm res}^{(ij)}$ as

$$\tau_{\rm res}^{(ij)} = \tau_{\rm meas}^{(ij)} - \sum_k \tau_k^{(ij)}, \tag{B1}$$

with associated 68% confidence level uncertainties obtained adding in quadrature the measurement errors and the uncertainties from the astrophysical contributions:

$$\sigma_x^2(\tau_{\rm res}^{(ij)}) = \sigma_x^2(\tau_{\rm meas}^{(ij)}) + \sum_k \sigma_x^2(\tau_k^{(ij)}), \tag{B2}$$

where the subscript x denotes whether these are upper- or lower-value errors—$\sigma_{\rm up}$ and $\sigma_{\rm low}$, respectively. We consider the cases for which $\tau_{\rm res}^{(ij)} < \sigma_{\rm low}(\tau_{\rm res}^{(ij)})$ (i.e., the low end of the 68% confidence level uncertainties lies below zero) as upper limits, set by

$$\sigma_{\rm up\ lim}(\tau_{\rm res}^{(ij)}) = ({\rm CDF}_{(ij)})^{-1}(0.683), \tag{B3}$$

which is the inverse of the cumulative distribution function of a normalized asymmetric Gaussian with only $\tau > 0$ and standard deviations given by $\sigma_{\rm up}(\tau_{\rm res}^{(ij)})$ and $\sigma_{\rm low}(\tau_{\rm res}^{(ij)})$, and consider $\tau_{\rm res}^{(ij)} = 0$.

Finally, we include the measured upper limits for the optical depth in our analysis, since they set a maximum to the contributions from unknown components of the EBL. In these cases, we consider $\tau_{\rm res}^{(ij)} = 0$, and the 68% confidence level upper limit to be

$$\sigma_{\rm up\ lim}^2(\tau_{\rm res}^{(ij)}) = \left(\sigma_{\rm up\ lim}(\tau_{\rm meas}^{(ij)}) - \sum_k \tau_k^{(ij)}\right)^2 + \sum_k \sigma_{\rm up}^2(\tau_k^{(ij)}). \tag{B4}$$

We subtract τ_k to the measured upper limit to take into account the fact that there is a *known* contribution below the detection limit. Therefore, additional contributions to the optical depth have to be added to that, after adding the astrophysical uncertainties in quadrature to the measured upper limit.

Once that we have the computed $\tau_{\rm res}^{(ij)}$ and its corresponding uncertainties, we can build the likelihood for additional contributions to the optical depth, which we denote with the subscript "extra." The value of $\tau_{\rm extra}$ depends on the parameters considered in each model, which we denote here with Θ. Following Ref. [46], we assume a Gaussian likelihood $\mathcal{L} \propto \exp(-\chi^2/2)$, considering that all measurements are uncorrelated, such as

$$\chi^2 = \begin{cases} \sum_{ij} \frac{(\tau_{\rm extra}^{(ij)}(\Theta) - \tau_{\rm res}^{(ij)})^2}{\sigma_{\rm up}^2(\tau_{\rm res}^{(ij)})} & \text{if } \tau_{\rm extra}^{(ij)}(\Theta) \geq \tau_{\rm res}^{(ij)}, \\ \sum_{ij} \frac{(\tau_{\rm extra}^{(ij)}(\Theta) - \tau_{\rm res}^{(ij)})^2}{\sigma_{\rm low}^2(\tau_{\rm res}^{(ij)})} & \text{if } \tau_{\rm extra}^{(ij)}(\Theta) < \tau_{\rm res}^{(ij)}, \\ \sum_{ij} \frac{(\tau_{\rm extra}^{(ij)}(\Theta))^2}{\sigma_{\rm up\ lim}^2(\tau_{\rm res}^{(ij)})} & \text{if } \tau_{\rm res}^{(ij)} = 0. \end{cases} \tag{B5}$$

Given that the maximum number of parameters that we consider in our models is two, we use a fine grid in parameter space to evaluate Eq. (B5), and obtain the unnormalized posterior distribution from $\Delta\chi^2(\Theta) \equiv \chi^2(\Theta) - \chi^2(\Theta_{\rm bf})$, where $\Theta_{\rm bf}$ are the best-fit parameter values.

APPENDIX C: NULL TESTS

Here we provide further comparison between the ALP case (the main case of study considered in this work) and two null tests. We focus on the EBL from galaxies at $z < 6$ since it is by far the dominant contribution. We consider (a) an overall boost of the astrophysical EBL from galaxies at $z < 6$, multiplying the standard contribution by $(1 + F_{\rm eEBL})$ factor; and (b) a potential underestimation of the EBL uncertainties, boosting the uncertainties of the contribution from galaxies at $z < 6$ by a constant factor.

1. ALPs vs $F_{\rm eEBL}$

We have shown in the main text that an overall 14–30% increase of the EBL can explain the optical depth excess with similar preference over the null hypothesis than ALP decays. Here we extend the comparison between the two hypotheses. In order to compare how well each case fit $\tau_{\rm res}$ we compare their χ^2 values for their best fit, defining a $\Delta\chi^2_{a-{\rm eEBL}} \equiv \chi^2_{a,{\rm bf}} - \chi^2_{\rm eEBL,bf}$; $\Delta\chi^2_{a-{\rm eEBL}} > 0$ denotes preference for the $F_{\rm eEBL}$ hypothesis and vice versa.

The results shown in Fig. 2 seem to indicate that $F_{\rm eEBL}$ and ALP decays fit better the more local and more distant blazars, respectively. We confirm this in Fig. 4, where we show $\Delta\chi^2_{a-{\rm eEBL}}$ for each bin in z_s and E_γ. While for most cases the two models perform similarly, there is a clear preference for ALPs at intermediate redshifts, while measurements at low redshifts and energies favor $F_{\rm eEBL}$. More quantitatively, we find $\Delta\chi^2_{a-{\rm eEBL}} = 0.79$ when considering all cases, which shifts to -2.9 if the first z_s bin is not considered in the whole analysis.

In Fig. 5 we show how the peak in the posterior at light masses disappears when the first z_s bin is removed. This proves that that peak was present only due to the first redshift bin (which, as shown in Fig. 2, does not fit satisfactorily. In this case, the best fit $F_{\rm eEBL} = 0.17$, is preferred over the null hypothesis at 1.9σ significance (p-value $= 5.6 \times 10^{-2}$). On the other hand, the best fit and significance for the ALP-decay case remains very similar. These results further support the scenario in which, if there are actually contributions from ALP decays, they may be

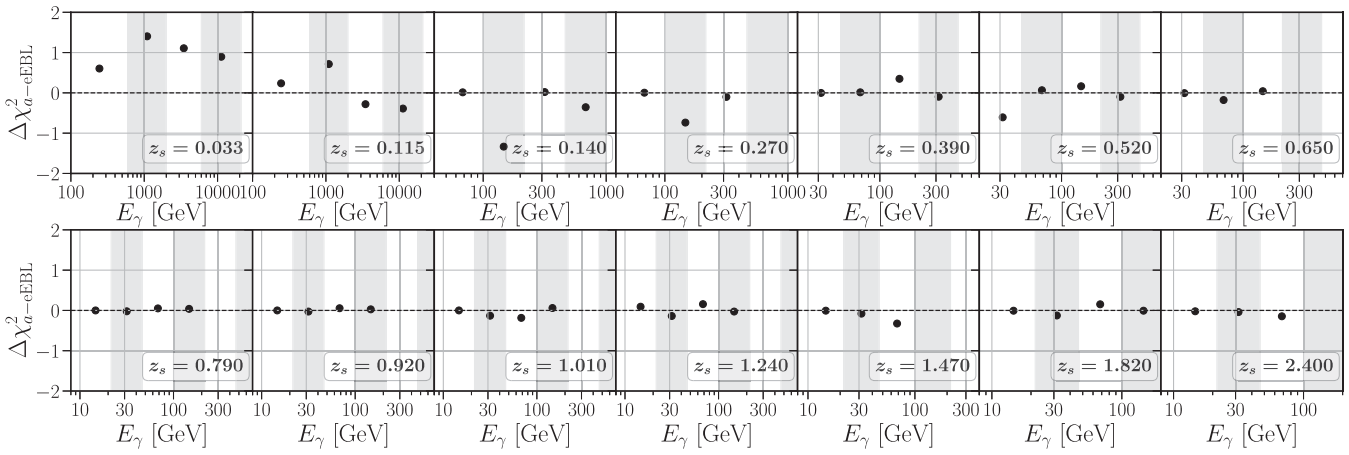

FIG. 4. Comparison of the individual χ^2 values for the best-fit cases in the ALP and F_{eEBL} scenarios.

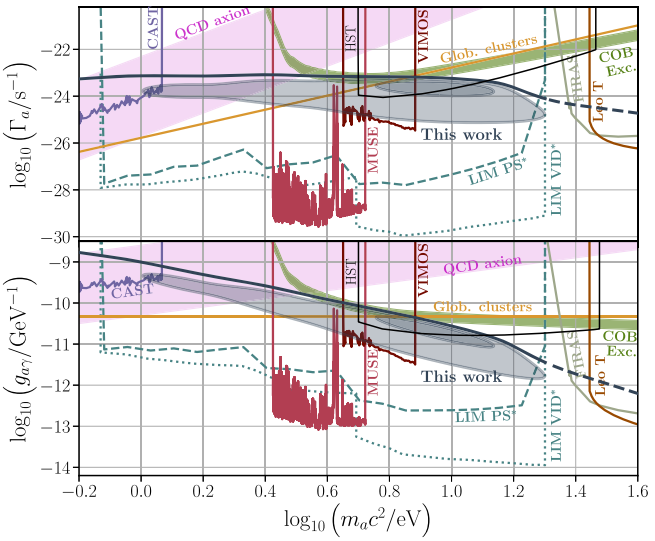

FIG. 5. Same as Fig. 3 but removing the first z_{s} bin from the analysis.

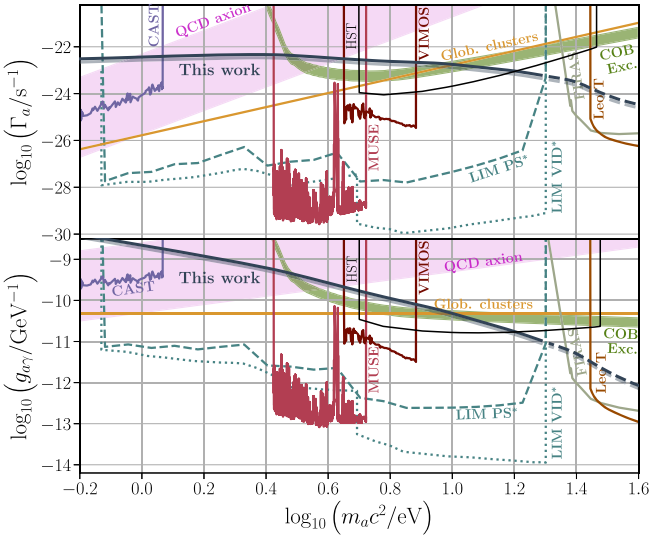

FIG. 6. 95% and 99% confidence level bounds on the ALP-photon effective coupling as function of mass from γ-ray attenuation for the extremely conservative scenario discussed in Appendix C 2 (dark blue lines, dashed lines denoting the masses that are affected by neutral hydrogen absorption), along with current strongest 95% confidence level bounds and preferred region to explain the COB excess, and the QCD axion band.

accompanied by additional astrophysical EBL to accomplish a good fit to both local and distant blazars.

2. Increasing EBL uncertainties

We carry out a final null test. In this case, we boost the uncertainties of the astrophysical EBL from galaxies at $z < 6$ by a constant factor until τ_{res} becomes an upper limit for all z_{s} and E_γ bins considered in the analysis. We find that the required factor is 14.36. By construction, in this case we do not find any preference for contributions from ALPs over the null hypothesis. However, we can set extremely conservative bounds on the ALP-photon effective coupling. We show the corresponding 95% and 99% confidence level bounds in Fig. 6. Even under these extremely conservative assumptions we find that the γ-ray attenuation significantly improves over current upper bounds by up to an order of magnitude. This result further motivates the study of γ-ray attenuation as a very promising probe of ALP and other exotic contributions to the EBL.

[1] A. Cooray, Extragalactic background light measurements and applications, R. Soc. Open Sci. **3**, 150555 (2016).
[2] G. Bertone, D. Hooper, and J. Silk, Particle dark matter: Evidence, candidates and constraints, Phys. Rep. **405**, 279 (2005).
[3] L. Abbott and P. Sikivie, A cosmological bound on the invisible axion, Phys. Lett. **120B**, 133 (1983).
[4] M. Dine and W. Fischler, The not-so-harmless axion, Phys. Lett. **120B**, 137 (1983).
[5] J. Preskill, M. B. Wise, and F. Wilczek, Cosmology of the invisible axion, Phys. Lett. **120B**, 127 (1983).
[6] S. Weinberg, A New Light Boson?, Phys. Rev. Lett. **40**, 223 (1978).
[7] F. Wilczek, Problem of Strong p and t Invariance in the Presence of Instantons, Phys. Rev. Lett. **40**, 279 (1978).
[8] R. D. Peccei and H. R. Quinn, CP Conservation in the Presence of Instantons, Phys. Rev. Lett. **38**, 1440 (1977).
[9] R. D. Peccei and H. R. Quinn, Constraints imposed by CP conservation in the presence of instantons, Phys. Rev. D **16**, 1791 (1977).
[10] D. J. E. Marsh, Axion cosmology, Phys. Rep. **643**, 1 (2016).
[11] J. Jaeckel, G. Rybka, and L. Winslow, Axion dark matter, arXiv:2203.14923.
[12] A. Caputo, C. P. Garay, and S. J. Witte, Looking for axion dark matter in dwarf spheroidals, Phys. Rev. D **98**, 083024 (2018); **99**, 089901(E) (2019).
[13] A. Caputo, M. Regis, M. Taoso, and S. J. Witte, Detecting the stimulated decay of axions at radiofrequencies, J. Cosmol. Astropart. Phys. 03 (2019) 027.
[14] Y. Gong, A. Cooray, K. Mitchell-Wynne, X. Chen, M. Zemcov, and J. Smidt, Axion decay and anisotropy of near-IR extragalactic background light, Astrophys. J. **825**, 104 (2016).
[15] A. Caputo, A. Vittino, N. Fornengo, M. Regis, and M. Taoso, Searching for axion-like particle decay in the near-infrared background: An updated analysis, J. Cosmol. Astropart. Phys. 05 (2021) 046.
[16] A. Caputo, M. Regis, and M. Taoso, Searching for sterile neutrino with x-ray intensity mapping, J. Cosmol. Astropart. Phys. 03 (2020) 001.
[17] A. Boyarsky, J. Franse, D. Iakubovskyi, and O. Ruchayskiy, Checking the Dark Matter Origin of a 3.53 keV Line with the Milky Way Center, Phys. Rev. Lett. **115**, 161301 (2015).
[18] S. Riemer-Sørensen, Constraints on the presence of a 3.5 keV dark matter emission line from Chandra observations of the galactic centre, Astron. Astrophys. **590**, A71 (2016).
[19] C. Dessert, N. L. Rodd, and B. R. Safdi, The dark matter interpretation of the 3.5-keV line is inconsistent with blank-sky observations, Science **367**, 1465 (2020).
[20] D. Cadamuro and J. Redondo, Cosmological bounds on pseudo Nambu-Goldstone bosons, J. Cosmol. Astropart. Phys. 02 (2012) 032.
[21] J. W. Foster, M. Kongsore, C. Dessert, Y. Park, N. L. Rodd, K. Cranmer, and B. R. Safdi, Deep Search for Decaying Dark Matter with XMM-Newton Blank-Sky Observations, Phys. Rev. Lett. **127**, 051101 (2021).
[22] A. Gewering-Peine, D. Horns, and J. H. M. M. Schmitt, A sensitive search for unknown spectral emission lines in the diffuse x-ray background with XMM-Newton, J. Cosmol. Astropart. Phys. 06 (2017) 036.
[23] C. Blanco and D. Hooper, Constraints on decaying dark matter from the isotropic gamma-ray background, J. Cosmol. Astropart. Phys. 03 (2019) 019.
[24] T. Cohen, K. Murase, N. L. Rodd, B. R. Safdi, and Y. Soreq, γ-ray Constraints on Decaying Dark Matter and Implications for IceCube, Phys. Rev. Lett. **119**, 021102 (2017).
[25] T. Nath Maity, A. K. Saha, A. Dubey, and R. Laha, Search for dark matter using sub-PeV γ-rays observed by Tibet AS_γ, Phys. Rev. D **105**, L041301 (2022).
[26] A. Esmaili and P. D. Serpico, First implications of Tibet AS_γ data for heavy dark matter, Phys. Rev. D **104**, L021301 (2021).
[27] J. Ellis, J. E. Kim, and D. V. Nanopoulos, Cosmological gravitino regeneration and decay, Phys. Lett. **145B**, 181 (1984).
[28] D. Wadekar and Z. Wang, Strong constraints on decay and annihilation of dark matter from heating of gas-rich dwarf galaxies, Phys. Rev. D **106**, 075007 (2022).
[29] W. Hu and J. Silk, Thermalization Constraints and Spectral Distortions for Massive Unstable Relic Particles, Phys. Rev. Lett. **70**, 2661 (1993).
[30] J. Chluba and R. A. Sunyaev, The evolution of CMB spectral distortions in the early Universe, Mon. Not. R. Astron. Soc. **419**, 1294 (2012).
[31] B. Bolliet, J. Chluba, and R. Battye, Spectral distortion constraints on photon injection from low-mass decaying particles, Mon. Not. R. Astron. Soc. **507**, 3148 (2021).
[32] F. Iocco, G. Mangano, G. Miele, O. Pisanti, and P. D. Serpico, Primordial nucleosynthesis: From precision cosmology to fundamental physics, Phys. Rep. **472**, 1 (2009).
[33] M. Pospelov and J. Pradler, Big bang nucleosynthesis as a probe of new physics, Annu. Rev. Nucl. Part. Sci. **60**, 539 (2010).
[34] V. Poulin and P. D. Serpico, Nonuniversal BBN bounds on electromagnetically decaying particles, Phys. Rev. D **91**, 103007 (2015).
[35] V. Poulin, P. D. Serpico, and J. Lesgourgues, A fresh look at linear cosmological constraints on a decaying Dark Matter component, J. Cosmol. Astropart. Phys. 08 (2016) 036.
[36] T. R. Slatyer, Indirect dark matter signatures in the cosmic dark ages. II. Ionization, heating, and photon production from arbitrary energy injections, Phys. Rev. D **93**, 023521 (2016).
[37] T. R. Slatyer and C.-L. Wu, General constraints on dark matter decay from the cosmic microwave background, Phys. Rev. D **95**, 023010 (2017).
[38] M. Lucca, N. Schöneberg, D. C. Hooper, J. Lesgourgues, and J. Chluba, The synergy between CMB spectral distortions and anisotropies, J. Cosmol. Astropart. Phys. 02 (2020) 026.
[39] J. V. Jelley, Absorption of high-energy gamma-rays within quasars and other radio sources, Nature (London) **211**, 472 (1966).

[40] R. J. Gould and G. P. Schreder, Pair production in photon-photon collisions, Phys. Rev. **155**, 1404 (1967).

[41] M. Ackermann, M. Ajello, A. Allafort, P. Schady, L. Baldini, J. Ballet *et al.*, The imprint of the extragalactic background light in the gamma-ray spectra of blazars, Science **338**, 1190 (2012).

[42] W. Essey, O. E. Kalashev, A. Kusenko, and J. F. Beacom, Secondary Photons and Neutrinos from Cosmic Rays Produced by Distant Blazars, Phys. Rev. Lett. **104**, 141102 (2010).

[43] W. Essey and A. Kusenko, A new interpretation of the gamma-ray observations of active galactic nuclei, Astropart. Phys. **33**, 81 (2010).

[44] W. Essey, O. Kalashev, A. Kusenko, and J. F. Beacom, Role of line-of-sight cosmic ray interactions in forming the spectra of distant blazars in TeV gamma rays and high-energy neutrinos, Astrophys. J. **731**, 51 (2011).

[45] J. D. Finke and S. Razzaque, Constraints on the extragalactic background light from very high energy gamma-ray observations of blazars, Astrophys. J. **698**, 1761 (2009).

[46] Fermi-LAT Collaboration, A γ-ray determination of the Universe's star formation history, Science **362**, 1031 (2018).

[47] V. A. Acciari, S. Ansoldi, L. A. Antonelli, A. Arbet Engels, D. Baack, A. Babić *et al.*, Measurement of the extragalactic background light using MAGIC and Fermi-LAT gamma-ray observations of blazars up to $z = 1$, Mon. Not. R. Astron. Soc. **486**, 4233 (2019).

[48] A. Desai, K. Helgason, M. Ajello, V. Paliya, A. Domínguez, J. Finke, and D. Hartmann, A GeV-TeV measurement of the extragalactic background light, Astrophys. J. Lett. **874**, L7 (2019).

[49] A. Domínguez, R. Wojtak, J. Finke, M. Ajello, K. Helgason, F. Prada, A. Desai, V. Paliya, L. Marcotulli, and D. H. Hartmann, A new measurement of the Hubble constant and matter content of the universe using extragalactic background light γ-ray attenuation, Astrophys. J. **885**, 137 (2019).

[50] R. C. Gilmore, Constraining the near-infrared background light from population III stars using high-redshift gamma-ray sources, Mon. Not. R. Astron. Soc. **420**, 800 (2012).

[51] J. Biteau and M. Meyer, Gamma-ray cosmology and tests of fundamental physics, Galaxies **10**, 39 (2022).

[52] D. Hooper and P. D. Serpico, Detecting Axion-Like Particles With Gamma Ray Telescopes, Phys. Rev. Lett. **99**, 231102 (2007).

[53] A. Mirizzi, G. G. Raffelt, and P. D. Serpico, Signatures of axionlike particles in the spectra of TeV gamma-ray sources, Phys. Rev. D **76**, 023001 (2007).

[54] K. A. Hochmuth and G. Sigl, Effects of axion-photon mixing on gamma-ray spectra from magnetized astrophysical sources, Phys. Rev. D **76**, 123011 (2007).

[55] A. de Angelis, M. Roncadelli, and O. Mansutti, Evidence for a new light spin-zero boson from cosmological gamma-ray propagation?, Phys. Rev. D **76**, 121301 (2007).

[56] A. Abramowski, F. Acero, F. Aharonian, F. Ait Benkhali, A. G. Akhperjanian, E. Angüner *et al.*, Constraints on axionlike particles with H.E.S.S. from the irregularity of the PKS 2155-304 energy spectrum, Phys. Rev. D **88**, 102003 (2013).

[57] M. Ajello, A. Albert, B. Anderson, L. Baldini, G. Barbiellini, D. Bastieri *et al.*, Search for Spectral Irregularities due to Photon-Axionlike-Particle Oscillations with the Fermi Large Area Telescope, Phys. Rev. Lett. **116**, 161101 (2016).

[58] H.-J. Li, J.-G. Guo, X.-J. Bi, S.-J. Lin, and P.-F. Yin, Limits on axionlike particles from Mrk 421 with 4.5-year period observations by ARGO-YBJ and Fermi-LAT, Phys. Rev. D **103**, 083003 (2021).

[59] S. Jacobsen, T. Linden, and K. Freese, Constraining axion-like particles with HAWC observations of TeV blazars, arXiv:2203.04332.

[60] H.-J. Li, Relevance of VHE blazar spectra models with axion-like particles, J. Cosmol. Astropart. Phys. 02 (2022) 025.

[61] H.-J. Li, Probing photon-ALP oscillations from the flat spectrum radio quasar $4C + 21.35$, Phys. Lett. B **829**, 137047 (2022).

[62] O. E. Kalashev, A. Kusenko, and E. Vitagliano, Cosmic infrared background excess from axionlike particles and implications for multimessenger observations of blazars, Phys. Rev. D **99**, 023002 (2019).

[63] A. Korochkin, A. Neronov, and D. Semikoz, Search for spectral features in extragalactic background light with gamma-ray telescopes, Astron. Astrophys. **633**, A74 (2020).

[64] A. Korochkin, A. Neronov, and D. Semikoz, Search for decaying eV-mass axion-like particles using gamma-ray signal from blazars, J. Cosmol. Astropart. Phys. 03 (2020) 064.

[65] T. R. Lauer, M. Postman, H. A. Weaver, J. R. Spencer, S. A. Stern, M. W. Buie *et al.*, New horizons observations of the cosmic optical background, Astrophys. J. **906**, 77 (2021).

[66] T. R. Lauer, M. Postman, J. R. Spencer, H. A. Weaver, S. A. Stern, G. R. Gladstone *et al.*, Anomalous flux in the cosmic optical background detected with new horizons observations, Astrophys. J. Lett. **927**, L8 (2022).

[67] A. Saldana-Lopez, A. Domínguez, P. G. Pérez-González, J. Finke, M. Ajello, J. R. Primack, J. R. Primack, V. S. Paliya, and A. Desai, An observational determination of the evolving extragalactic background light from the multiwavelength HST/CANDELS survey in the Fermi and CTA era, Mon. Not. R. Astron. Soc. **507**, 5144 (2021).

[68] J. L. Bernal, G. Sato-Polito, and M. Kamionkowski, The Cosmic Optical Background Excess, Dark Matter, and Line-Intensity Mapping, Phys. Rev. Lett. **129**, 231301 (2022).

[69] C. Creque-Sarbinowski and M. Kamionkowski, Searching for decaying and annihilating dark matter with line intensity mapping, Phys. Rev. D **98**, 063524 (2018).

[70] J. L. Bernal, A. Caputo, and M. Kamionkowski, Strategies to detect dark-matter decays with line-intensity mapping, Phys. Rev. D **103**, 063523 (2021).

[71] M. Shirasaki, Searching for eV-mass axionlike particles with cross correlations between line intensity and weak lensing maps, Phys. Rev. D **103**, 103014 (2021).

[72] J. Biteau and D. A. Williams, The extragalactic background light, the Hubble constant, and anomalies: Conclusions from 20 years of TeV gamma-ray observations, Astrophys. J. **812**, 60 (2015).
[73] K. Mattila, P. Väisänen, K. Lehtinen, G. von Appen-Schnur, and C. Leinert, Extragalactic background light: A measurement at 400 nm using dark cloud shadow—II. Spectroscopic separation of the dark cloud's light, and results*, Mon. Not. R. Astron. Soc. **470**, 2152 (2017).
[74] S. Matsuura, T. Arai, J. J. Bock, A. Cooray, P. M. Korngut, M. G. Kim *et al.*, New spectral evidence of an unaccounted component of the near-infrared extragalactic background light from the CIBER, Astrophys. J. **839**, 7 (2017).
[75] Y. Matsuoka, N. Ienaka, K. Kawara, and S. Oyabu, Cosmic optical background: The view from pioneer 10/11, Astrophys. J. **736**, 119 (2011).
[76] T. Matsumoto, K. Tsumura, Y. Matsuoka, and J. Pyo, Zodiacal light beyond earth orbit observed with pioneer 10, Astron. J. **156**, 86 (2018).
[77] M. Zemcov, P. Immel, C. Nguyen, A. Cooray, C. M. Lisse, and A. R. Poppe, Measurement of the cosmic optical background using the long range reconnaissance imager on new horizons, Nat. Commun. **8**, 15003 (2017).
[78] A. Cooray, J. Smidt, F. de Bernardis, Y. Gong, D. Stern, M. L. N. Ashby *et al.*, Near-infrared background anisotropies from diffuse intrahalo light of galaxies, Nature (London) **490**, 514 (2012).
[79] M. Zemcov, J. Smidt, T. Arai, J. Bock, A. Cooray, Y. Gong *et al.*, On the origin of near-infrared extragalactic background light anisotropy, Science **346**, 732 (2014).
[80] T. Matsumoto and K. Tsumura, Fluctuation of the background sky in the Hubble extremely deep field (XDF) and its origin, Publ. Astron. Soc. Jpn. **71**, 88 (2019).
[81] J. D. Finke, S. Razzaque, and C. D. Dermer, Modeling the extragalactic background light from stars and dust, Astrophys. J. **712**, 238 (2010).
[82] A. Domínguez, J. R. Primack, D. J. Rosario, F. Prada, R. C. Gilmore, S. M. Faber *et al.*, Extragalactic background light inferred from AEGIS galaxy-SED-type fractions, Mon. Not. R. Astron. Soc. **410**, 2556 (2011).
[83] K. Helgason and A. Kashlinsky, Reconstructing the γ-ray photon optical depth of the universe to z ~ 4 from multiwavelength galaxy survey data, Astrophys. J. Lett. **758**, L13 (2012).
[84] R. C. Gilmore, R. S. Somerville, J. R. Primack, and A. Domínguez, Semi-analytic modelling of the extragalactic background light and consequences for extragalactic gamma-ray spectra, Mon. Not. R. Astron. Soc. **422**, 3189 (2012).
[85] S. P. Driver, S. K. Andrews, L. J. Davies, A. S. G. Robotham, A. H. Wright, R. A. Windhorst, S. Cohen, K. Emig, R. A. Jansen, and L. Dunne, Measurements of extragalactic background light from the far UV to the far IR from deep ground- and space-based galaxy counts, Astrophys. J. **827**, 108 (2016).
[86] F. W. Stecker, S. T. Scully, and M. A. Malkan, An empirical determination of the intergalactic background light from UV to FIR wavelengths using FIR deep galaxy surveys and the gamma-ray opacity of the universe, Astrophys. J. **827**, 6 (2016); **863**, 112(E) (2018).
[87] N. A. Grogin, D. D. Kocevski, S. M. Faber, H. C. Ferguson, A. M. Koekemoer, A. G. Riess *et al.*, CANDELS: The cosmic assembly near-infrared deep extragalactic legacy survey, Astrophys. J. Suppl. Ser. **197**, 35 (2011).
[88] A. M. Koekemoer, S. M. Faber, H. C. Ferguson, N. A. Grogin, D. D. Kocevski, D. C. Koo *et al.*, CANDELS: The cosmic assembly near-infrared deep extragalactic legacy survey—The Hubble space telescope observations, imaging data products, and mosaics, Astrophys. J. Suppl. Ser. **197**, 36 (2011).
[89] N. Aghanim *et al.* (Planck Collaboration), Planck 2018 results. VI. Cosmological parameters, Astron. Astrophys. **641**, A6 (2020); **652**, C4(E) (2021).
[90] J. Mirocha, Decoding the x-ray properties of pre-reionization era sources, Mon. Not. R. Astron. Soc. **443**, 1211 (2014).
[91] J. Mirocha, S. R. Furlanetto, and G. Sun, The global 21-cm signal in the context of the high- z galaxy luminosity function, Mon. Not. R. Astron. Soc. **464**, 1365 (2017).
[92] J. Mirocha, R. H. Mebane, S. R. Furlanetto, K. Singal, and D. Trinh, Unique signatures of Population III stars in the global 21-cm signal, Mon. Not. R. Astron. Soc. **478**, 5591 (2018).
[93] J. E. Krick and R. A. Bernstein, Diffuse optical light in galaxy clusters II: Correlations with cluster properties, Astron. J. **134**, 466 (2007).
[94] K. Mitchell-Wynne *et al.*, Ultraviolet luminosity density of the universe during the epoch of reionization, Nat. Commun. **6**, 7945 (2015).
[95] N. Blinov, M. J. Dolan, P. Draper, and J. Kozaczuk, Dark matter targets for axionlike particle searches, Phys. Rev. D **100**, 015049 (2019).
[96] P. Arias, D. Cadamuro, M. Goodsell, J. Jaeckel, J. Redondo, and A. Ringwald, WISPy cold dark matter, J. Cosmol. Astropart. Phys. 06 (2012) 013.
[97] C. Eröncel, R. Sato, G. Servant, and P. Sørensen, ALP dark matter from kinetic fragmentation: Opening up the parameter window, J. Cosmol. Astropart. Phys. 10 (2022) 053.
[98] M. Farina, D. Pappadopulo, F. Rompineve, and A. Tesi, The photo-philic QCD axion, J. High Energy Phys. 01 (2017) 095.
[99] CAST Collaboration, New CAST limit on the axion-photon interaction, Nat. Phys. **13**, 584 (2017).
[100] D. Grin, G. Covone, J.-P. Kneib, M. Kamionkowski, A. Blain, and E. Jullo, A telescope search for decaying relic axions, Phys. Rev. D **75**, 105018 (2007).
[101] M. Regis, M. Taoso, D. Vaz, J. Brinchmann, S. L. Zoutendijk, N. Bouché, and M. Steinmetz, Searching for light in the darkness: Bounds on ALP dark matter with the optical MUSE-Faint survey, Phys. Lett. B **814**, 136075 (2021).
[102] A. Ayala, I. Domínguez, M. Giannotti, A. Mirizzi, and O. Straniero, Revisiting the Bound on Axion-Photon Coupling from Globular Clusters, Phys. Rev. Lett. **113**, 191302 (2014).
[103] M. J. Dolan, F. J. Hiskens, and R. R. Volkas, Advancing globular cluster constraints on the axion-photon coupling, J. Cosmol. Astropart. Phys. 10 (2022) 096.

[104] K. Nakayama and W. Yin, Anisotropic cosmic optical background bound for decaying dark matter in light of the LORRI anomaly, Phys. Rev. D **106**, 103505 (2022).
[105] D. Cadamuro and J. Redondo, Cosmological bounds on pseudo Nambu-Goldstone bosons, J. Cosmol. Astropart. Phys. 02 (2012) 032.
[106] B. S. Acharya *et al.* (CTA Consortium Collaboration), *Science with the Cherenkov Telescope Array* (World Scientific Publishing, Singapore, 2018).
[107] R. A. Windhorst *et al.*, SKYSURF: Constraints on zodiacal light and extragalactic background light through panchromatic HST All-Sky surface-brightness measurements: I. Survey overview and methods, Astron. J. **164**, 141 (2022).
[108] O. Doré, J. Bock, M. Ashby, P. Capak, A. Cooray *et al.*, Cosmology with the SPHEREX all-sky spectral survey, arXiv:1412.4872.
[109] J. L. Bernal, A. Caputo, F. Villaescusa-Navarro, and M. Kamionkowski, Searching for the Radiative Decay of the Cosmic Neutrino Background with Line-Intensity Mapping, Phys. Rev. Lett. **127**, 131102 (2021).
[110] R. J. Bouwens, G. D. Illingworth, P. A. Oesch, M. Trenti, I. Labbé, L. Bradley *et al.*, UV luminosity functions at redshifts $z \sim 4$ to $z \sim 10$: 10,000 galaxies from HST legacy fields, Astrophys. J. **803**, 34 (2015).
[111] J. J. Eldridge and E. R. Stanway, Spectral population synthesis including massive binaries, Mon. Not. R. Astron. Soc. **400**, 1019 (2009).
[112] D. Schaerer, The transition from Population III to normal galaxies: Lyalpha and He II emission and the ionising properties of high redshift starburst galaxies, Astron. Astrophys. **397**, 527 (2003).
[113] G. Sun, J. Mirocha, R. H. Mebane, and S. R. Furlanetto, Revealing the formation histories of the first stars with the cosmic near-infrared background, Mon. Not. R. Astron. Soc. **508**, 1954 (2021).
[114] K. Mitsuda, H. Inoue, K. Koyama, K. Makishima, M. Matsuoka, Y. Ogawara *et al.*, Energy spectra of low-mass binary x-ray sources observed from Tenma, Publ. Astron. Soc. Jpn. **36**, 741 (1984).
[115] S. Mineo, M. Gilfanov, and R. Sunyaev, X-ray emission from star-forming galaxies—I. High-mass x-ray binaries, Mon. Not. R. Astron. Soc. **419**, 2095 (2012).
[116] C. Conroy, R. H. Wechsler, and A. V. Kravtsov, The hierarchical build-up of massive galaxies and the intracluster light since $z = 1$, Astrophys. J. **668**, 826 (2007).
[117] A. Cooray, J. Smidt, F. De Bernardis, Y. Gong, D. Stern, M. L. N. Ashby *et al.*, A measurement of the intrahalo light fraction with near-infrared background anisotropies, Nature (London) **494**, 514 (2012).
[118] J. L. Tinker, A. V. Kravtsov, A. Klypin, K. Abazajian, M. S. Warren, G. Yepes, S. Gottlöber, and D. E. Holz, Toward a halo mass function for precision cosmology: The limits of universality, Astrophys. J. **688**, 709 (2008).
[119] Y.-T. Lin, J. J. Mohr, and S. A. Stanford, K-band properties of galaxy clusters and groups: Luminosity function, radial distribution and halo occupation number, Astrophys. J. **610**, 745 (2004).
[120] M. Polletta *et al.*, Spectral energy distributions of hard x-ray selected AGNs in the XMDS survey, Astrophys. J. **663**, 81 (2007).